

New New-Phenomena Results from D \emptyset *

Jianming Qian

Department of Physics, Univ. of Michigan, Ann Arbor, MI 48109, USA

E-mail: qianj@umich.edu

(for the D \emptyset Collaboration)

We have searched for diphoton events ($\gamma\gamma E_T$) with large missing transverse momentum, γE_T events ($\gamma E_T + \geq 2$ jets) with two or more jets, and diphoton events ($\gamma\gamma$) with high transverse energies in $p\bar{p}$ collisions at $\sqrt{s} = 1.8$ TeV using approximately 100 pb^{-1} of data collected with the D \emptyset detector at the Fermilab Tevatron in 1992–1996. No excess of events beyond the expected backgrounds is observed. The null results are interpreted in supersymmetric models with a dominant $\tilde{\chi}_2^0 \rightarrow \gamma\tilde{\chi}_1^0$ decay and in terms of Dirac pointlike monopole production.

*Presented at the 1998 Rencontres de Physique de la Vallée d’Aoste on Results and Perspectives in Particle Physics, La Thuile, Italy, March 1–7, 1998.

I. INTRODUCTION

The DØ detector collected a data sample corresponding to an integrated luminosity of approximately 100 pb^{-1} during the 1992–1996 Tevatron Run at $\sqrt{s} = 1.8 \text{ GeV}$. The detector consists of three major components: a non-magnetic tracking system including a transition radiation detector in the central region, a liquid-argon calorimeter, and a toroidal magnetic muon spectrometer. A detailed description of the DØ detector can be found in Ref. [1]. The Tevatron $p\bar{p}$ collider is ideal for studying high p_T phenomena. It is a natural place to search for new physics beyond the Standard Model. In this talk, the results of the searches for supersymmetry and Dirac monopoles are presented.

II. SEARCH FOR SUPERSYMMETRY USING PHOTONS

Supersymmetry [2] is a generalization of space-time symmetry. It introduces for every Standard Model particle a supersymmetric partner that differs in spin by $1/2$. \mathcal{R} -parity conservation requires that supersymmetric particles be produced in pairs and that the lightest supersymmetric particle (LSP) be stable.

The minimal supersymmetric standard model (MSSM) is the simplest supersymmetric model. In the MSSM, the Gaugino-Higgsino sector (excluding gluinos) is described by four parameters: M_1 , M_2 , μ , and $\tan\beta$, where M_1 and M_2 are the $U(1)$ and $SU(2)$ gaugino mass parameters, μ is the Higgsino mass parameter, and $\tan\beta$ is the ratio of the vacuum expectation values of the two Higgs doublets. The Gaugino-Higgsino mixing gives in four neutral mass eigenstates (neutralinos $\tilde{\chi}_i^0$, $i = 1, 2, 3, 4$) and two charged mass eigenstates (charginos $\tilde{\chi}_j^\pm$, $j = 1, 2$) whose masses and couplings are fixed by the above four parameters. Supersymmetric models [3,4] predicting photon production have been proposed as possible explanations of a recent event [5] reported by the CDF collaboration. Within the MSSM, it has been shown that the radiative decay of $\tilde{\chi}_2^0 \rightarrow \tilde{\gamma}\chi_1^0$ dominates in some regions of parameter space [6]. Assuming $\tilde{\chi}_1^0$ is the LSP, the production of $\tilde{\chi}_2^0$, either directly or indirectly from decays of other supersymmetry particles, will result in events with two high transverse energy (E_T) photons and large missing transverse momentum (\cancel{E}_T) and/or in events ($\gamma\cancel{E}_T + n$ jets) with one high E_T photon, multile jets and large \cancel{E}_T . Moreover, the $\gamma\gamma\cancel{E}_T$ events are also expected in supersymmetric models with a light gravitino (\tilde{G}) being the LSP. In this case, $\tilde{\chi}_1^0$ (assumed to be the lightest superpartner of a standard model particle) is unstable and decays into a photon plus a gravitino ($\tilde{\chi}_1^0 \rightarrow \gamma\tilde{G}$).

We present searches for new physics in the channels $p\bar{p} \rightarrow \gamma\gamma\cancel{E}_T + X$ and $p\bar{p} \rightarrow \gamma\cancel{E}_T + \geq 2$ jets + X at the Fermilab Tevatron. The $\gamma\cancel{E}_T$ events with fewer than two jets are not considered here, due to large backgrounds from W +jets production. We interpret our results of the $\gamma\gamma\cancel{E}_T$ analysis in terms of $\tilde{e}\tilde{e}$, $\tilde{\nu}\tilde{\nu}$, and $\tilde{\chi}_2^0\tilde{\chi}_2^0$ production and of the $\gamma\cancel{E}_T + \geq 2$ jets analysis in terms of squark (\tilde{q}) and gluino (\tilde{g}) production in supersymmetric models with a dominant $\tilde{\chi}_2^0 \rightarrow \gamma\tilde{\chi}_1^0$ decay. The interpretation of the results of the $\gamma\gamma\cancel{E}_T$ analysis in models with a light \tilde{G} can be found in Ref. [7].

The trigger used requires one electromagnetic (EM) cluster with transverse energy $E_T > 15 \text{ GeV}$, one jet with $E_T > 10 \text{ GeV}$, and $\cancel{E}_T > 14 \text{ GeV}$ ($\cancel{E}_T > 10 \text{ GeV}$ for about 10% of the data taken early in the Tevatron run). The jets in the trigger include non-leading EM

clusters. Photons are identified via a two-step process: the selection of isolated EM energy clusters and the rejection of electrons. The EM clusters are selected from calorimeter energy clusters by requiring (i) at least 95% of the energy to be deposited in the EM section of the calorimeter, (ii) the transverse and longitudinal shower profiles to be consistent with those expected for an EM shower, and (iii) the energy in an annular isolation cone with radius 0.2 to 0.4 around the cluster in $\eta - \phi$ space to be less than 10% of the cluster energy, where η and ϕ are the pseudorapidity and azimuthal angle. Electrons are removed by rejecting EM clusters which have either a reconstructed track or a large number of tracking chamber hits in a road between the calorimeter cluster and the event vertex. \cancel{E}_T is determined from the energy deposition in the calorimeter for $|\eta| < 4.5$.

A. Search for $\gamma\gamma\cancel{E}_T$ Events

To be selected as $\gamma\gamma\cancel{E}_T$ candidates, events are first required to have two identified photons, one with $E_T^{\gamma 1} > 20$ GeV and the other with $E_T^{\gamma 2} > 12$ GeV, each with pseudorapidity $|\eta^\gamma| < 1.1$ or $1.5 < |\eta^\gamma| < 2.0$, the regions with good photon identification. We denote the 28 events passing these photon requirements as the $\gamma\gamma$ sample. We then require $\cancel{E}_T > 25$ GeV with at least one reconstructed vertex in the event to ensure good measurement of \cancel{E}_T . No requirement on jets is made. Two events satisfy all requirements. The data used in this analysis correspond to an integrated luminosity of 106.3 ± 5.6 pb $^{-1}$.

The principal backgrounds are multijet, direct photon, $W + \gamma$, $W +$ jets, $Z \rightarrow ee$, and $Z \rightarrow \tau\tau \rightarrow ee$ events from Standard Model processes with misidentified photons and/or mismeasured \cancel{E}_T . The background due to \cancel{E}_T mismeasurement is estimated using events with two EM-like clusters which satisfy looser EM cluster requirements than those discussed above, and for which at least one of the two fails the EM shower profile consistency requirement (ii) above. In addition, these events must pass the photon kinematic requirements. By normalizing the number of events with $\cancel{E}_T < 20$ GeV in the QCD sample to that in the $\gamma\gamma$ sample, we obtain a background of 2.1 ± 0.9 events due to \cancel{E}_T mismeasurement for $\cancel{E}_T > 25$ GeV.

Other backgrounds are due to events with genuine \cancel{E}_T such as those from $W + \gamma$ (where ‘ γ ’ can be a real or a fake photon), $Z \rightarrow \tau\tau \rightarrow ee$, and $t\bar{t} \rightarrow ee +$ jets production. These events would fake $\gamma\gamma\cancel{E}_T$ events if the electrons were misidentified as photons. We estimate their contribution using a sample of $e + \gamma$ events passing the kinematic requirements, including that on \cancel{E}_T . Taking into account the probability (0.0045 ± 0.0008 , determined from $Z \rightarrow ee$ data) that an electron is misidentified as a photon, we estimate a background of 0.2 ± 0.1 events. Adding the two background contributions together yields 2.3 ± 0.9 events. No excess of events is observed.

The null results are used to set upper cross section limits on the pair production of scalar electron (\tilde{e}), scalar neutrino ($\tilde{\nu}$), and $\tilde{\chi}_2^0$ with $\text{Br}(\tilde{e} \rightarrow e\tilde{\chi}_2^0) = 100\%$, $\text{Br}(\tilde{\nu} \rightarrow \nu\tilde{\chi}_2^0) = 100\%$, and $\text{Br}(\tilde{\chi}_2^0 \rightarrow \gamma\tilde{\chi}_1^0) = 100\%$. $p\bar{p} \rightarrow \tilde{e}\tilde{e}, \tilde{\nu}\tilde{\nu}, \tilde{\chi}_2^0\tilde{\chi}_2^0$ events are generated using the ISAJET program [8] and are processed through the detector and trigger simulation and the reconstruction program. The \tilde{e} mass is set to 100 GeV/c 2 while the $\tilde{\nu}$, $\tilde{\chi}_2^0$, and $\tilde{\chi}_1^0$ masses are varied between 70–100 GeV/c 2 , 50–90 GeV/c 2 , and 30–80 GeV/c 2 respectively. The efficiency is found to be insensitive to the \tilde{e} and $\tilde{\nu}$ masses and is largely determined by

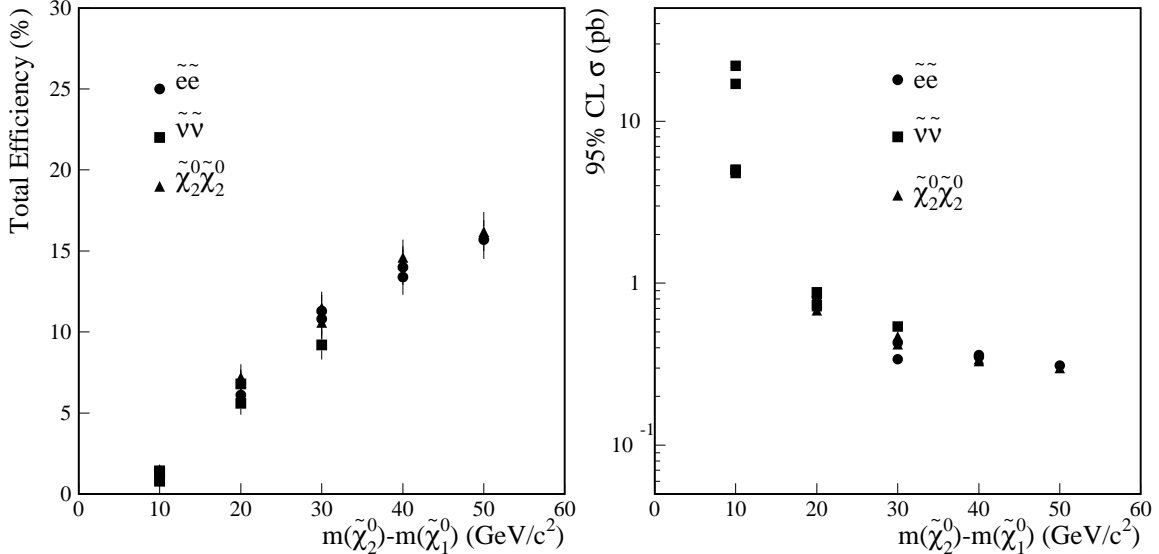


FIG. 1. (a) The total efficiency and (b) the 95% C.L. cross section limit as a function of $m_{\tilde{\chi}_2^0} - m_{\tilde{\chi}_1^0}$ for $p\bar{p} \rightarrow \tilde{e}\tilde{e}, \tilde{\nu}\tilde{\nu}, \tilde{\chi}_2^0\tilde{\chi}_2^0$ processes. The error shown on the efficiency is statistical only and the systematic error is estimated to be 6%.

the mass difference $m_{\tilde{\chi}_2^0} - m_{\tilde{\chi}_1^0}$ as shown in Fig. 1(a). For a given value of $m_{\tilde{\chi}_2^0} - m_{\tilde{\chi}_1^0}$, the efficiencies for the three processes are the same within the errors, independent of the values of $m_{\tilde{e}}$, $m_{\tilde{\nu}}$, and $m_{\tilde{\chi}_2^0}$. The 95% confidence level (C.L.) upper limits on the cross section as a function of $m_{\tilde{\chi}_2^0} - m_{\tilde{\chi}_1^0}$ is shown in Fig. 1(b). The limit is about 300 fb for large values of $m_{\tilde{\chi}_2^0} - m_{\tilde{\chi}_1^0}$. These results improve over those we published earlier [9], mainly due to the improved photon identification. However, we note that the expected cross sections for $p\bar{p} \rightarrow \tilde{e}\tilde{e}, \tilde{\nu}\tilde{\nu}, \tilde{\chi}_2^0\tilde{\chi}_2^0$ processes are small, well below the experimental upper limits. For example, the theoretical cross section for $p\bar{p} \rightarrow \tilde{e}_L\tilde{e}_L + \tilde{e}_R\tilde{e}_R$ production is about 30 fb for $m_{\tilde{e}} = 100$ GeV/c².

B. Search for $\gamma\cancel{E}_T + n$ Jets Events

To be selected as $\gamma\cancel{E}_T + \geq 2$ jets candidates, events are first required to have at least one identified photon with $E_T^\gamma > 20$ GeV and pseudorapidity $|\eta^\gamma| < 1.1$ or $1.5 < |\eta^\gamma| < 2.0$, and two or more jets with $E_T^j > 20$ GeV and $|\eta^j| < 2.0$. We denote events passing these requirements as the $\gamma + \geq 2$ jets sample. The \cancel{E}_T distribution of the $\gamma + \geq 2$ jets events is shown in Fig. 2(a). After requiring $\cancel{E}_T > 25$ GeV, 378 events remain in the sample. The data used in this analysis correspond to an integrated luminosity of 99.4 ± 5.4 pb⁻¹.

The principal backgrounds are multijet, direct photon, $W +$ jets, and $Z +$ jets events from Standard Model processes with jets or electrons misidentified as photons and/or mismeasured \cancel{E}_T . Following the same procedure as in the $\gamma\gamma\cancel{E}_T$ analysis, the background due to \cancel{E}_T mismeasurement is estimated to be 370 ± 36 events. $W + \geq 2$ jets events with $W \rightarrow e\nu$ would fake $\gamma\cancel{E}_T + \geq 2$ jets events if the electrons were misidentified as photons. This contribution is estimated to be 4 ± 1 using a sample of $e\cancel{E}_T + \geq 2$ jets events passing all the kinematic requirements with the electron satisfying those imposed on the photon. Another

background due to $W(\rightarrow \ell\nu) + \text{jets}$ and $Z(\rightarrow \nu\nu) + \text{jets}$ production is found to be negligible. The total background (374 ± 36) agrees well with the number of observed events. The H_T (defined as the scalar sum of the E_T of all jets with $E_T > 20$ GeV and $|\eta| < 2.0$) distribution is shown in Fig. 2(b) for both $\gamma\cancel{E}_T + \geq 2$ jets and background samples. The background distribution reproduces the observed $\gamma\cancel{E}_T + \geq 2$ jets distribution well.

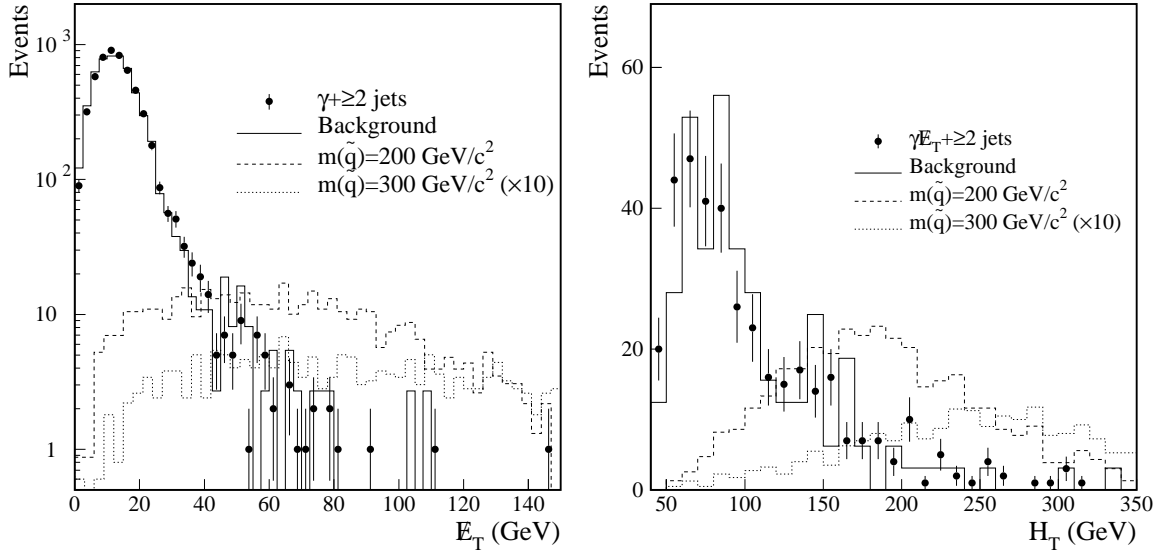


FIG. 2. (a) The \cancel{E}_T distribution (solid circles) of the events with one photon and two or more jets. The expected \cancel{E}_T distribution from the backgrounds is shown as a solid histogram. The number of events with $\cancel{E}_T < 20$ GeV in the background is normalized to that in the $\gamma + \geq 2$ jets sample. (b) The H_T distributions of the $\gamma\cancel{E}_T + \geq 2$ jets and background events. Also shown (dashed and dotted histograms) are the expected distributions from supersymmetry for two different values of squark/gluino masses assuming an equal squark and gluino mass.

With the basic selection discussed above, the $\gamma\cancel{E}_T + \geq 2$ jets sample is dominated by the backgrounds. To optimize the selection criteria for supersymmetry, we simulate squark and gluino production (either in pair or in association with charginos/neutralinos) using the PYTHIA program [10]. The MSSM parameter values are set to $M_1 = M_2 = 60.0$ GeV, $\tan\beta = 2.0$, and $\mu = -40.0$ GeV. This set of parameter values gives $m_{\tilde{\chi}_1^0} = 33.5$ GeV/c², $m_{\tilde{\chi}_2^0} = 60.0$ GeV/c², and $\text{Br}(\tilde{\chi}_2^0 \rightarrow \gamma\tilde{\chi}_1^0) = 100\%$. Sleptons ($\tilde{\ell}$) and stop (\tilde{t}) are assumed to be heavy. Events with $\tilde{\chi}_2^0$ in the final state are selected and are run through a detector simulation program, a trigger simulator, and the same trigger requirements, reconstruction, and analysis as the data. The \cancel{E}_T and H_T distributions for $m_{\tilde{q}}(= m_{\tilde{g}}) = 200, 300$ GeV/c² events after the basic selection are shown in Figs. 2. The distributions expected from supersymmetry are considerably harder than those of the background events. To increase sensitivity to supersymmetry, we introduce an H_T cut and maximize the ϵ/σ_b ratio by varying \cancel{E}_T and H_T requirements. Here ϵ is the efficiency for $m_{\tilde{q}}(= m_{\tilde{g}}) = 300$ GeV/c² MC events and σ_b is the error on the estimated number of background events. The optimized cuts are found to be $\cancel{E}_T > 45$ GeV and $H_T > 220$ GeV. With these additional cuts, five $\gamma\cancel{E}_T + \geq 2$ jets events are observed while 8 ± 6 events are expected from the background processes.

The efficiency for supersymmetry signal varies from a few percent for low mass \tilde{q}/\tilde{g} to

approximately 25% for high mass \tilde{q}/\tilde{g} . MC studies show that the efficiency varies by 4% for different choices of M_1 , M_2 , $\tan\beta$, and μ which are consistent with $\text{Br}(\tilde{\chi}_2^0 \rightarrow \gamma\tilde{\chi}_1^0) = 100\%$ and $m_{\tilde{\chi}_2^0} - m_{\tilde{\chi}_1^0} > 20 \text{ GeV}/c^2$ suggested in Ref. [4]. Experimentally, the mass requirement is needed to ensure that photons from $\tilde{\chi}_2^0$ decays are reasonably energetic and are detected with good efficiency. The variation is assigned as a systematic error in the efficiency. The total fractional systematic error on the efficiency is 9%.

With five events observed and 8 ± 6 events expected from backgrounds, we observe no excess of events. We compute 95% C.L. upper limits on $\sigma \times \text{Br} = \sigma(p\bar{p} \rightarrow \tilde{q}/\tilde{g} \rightarrow \tilde{\chi}_2^0 + X) \times \text{Br}(\tilde{\chi}_2^0 \rightarrow \gamma\tilde{\chi}_1^0)$ using a Bayesian approach with a flat prior distribution for the signal cross section. The resulting upper limit as a function of squark/gluino mass is displayed in Fig. 3, for the case where $m_{\tilde{q}} = m_{\tilde{g}}$, along with the theoretical cross sections, as calculated using the CTEQ3L parton distribution function (p.d.f.) [11]. The hatched band represents the range of the theoretical cross sections obtained by varying the supersymmetry parameter values with the constraints $\text{Br}(\tilde{\chi}_2^0 \rightarrow \gamma\tilde{\chi}_1^0) = 100\%$ and $m_{\tilde{\chi}_2^0} - m_{\tilde{\chi}_1^0} > 20 \text{ GeV}/c^2$. The intersection of our limit curve with the lower edge of the theory band is at $\sigma \times \text{Br} = 0.38 \text{ pb}$, leading to a lower limit for equal mass squarks and gluinos of $311 \text{ GeV}/c^2$.

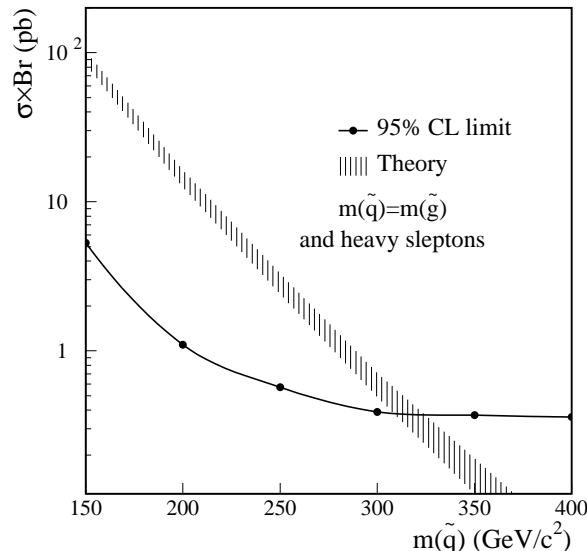


FIG. 3. The 95% C.L. upper limit on the $\sigma \times \text{Br}$ as a function of $m_{\tilde{q}/\tilde{g}}$ assuming an equal squark and gluino mass. The hatched band represents the range of the theoretical cross section for different sets of MSSM parameter values consistent with the constraints $\text{Br}(\tilde{\chi}_2^0 \rightarrow \gamma\tilde{\chi}_1^0) = 100\%$ and $m_{\tilde{\chi}_2^0} - m_{\tilde{\chi}_1^0} > 20 \text{ GeV}/c^2$.

The effect of light sleptons on the squark and gluino decays is studied by varying the slepton mass ($m_{\tilde{\ell}}$) in MC. The fraction of events containing at least one $\tilde{\chi}_2^0$ increases as the $m_{\tilde{\ell}}$ is decreased. When $m_{\tilde{\ell}}$ is varied from $500 \text{ GeV}/c^2$ to $80 \text{ GeV}/c^2$, the fraction increases about 25% for $m_{\tilde{q}} = m_{\tilde{g}} = 300 \text{ GeV}/c^2$ with equal gluino mass. Sleptons with mass below $80 \text{ GeV}/c^2$ have already been excluded [12]. The increased $\tilde{\chi}_2^0$ production increases the mass limit by approximately $10 \text{ GeV}/c^2$.

A light stop (\tilde{t}_1) will also modify the squark and gluino decays and therefore affect the $\tilde{\chi}_2^0$ production. We investigate this effect by setting $m_{\tilde{t}_1} = 80 \text{ GeV}/c^2$ which approximately

corresponds to the current \tilde{t}_1 lower mass limit [12]. A 15% reduction in $\tilde{\chi}_2^0$ production cross section is observed. This reduction lowers the limit for equal mass squarks and gluinos by about $6 \text{ GeV}/c^2$.

Following the procedure above, we obtain a low mass limit for gluinos (squarks) to be $233 \text{ GeV}/c^2$ ($219 \text{ GeV}/c^2$) when squarks (gluinos) are heavy. Again, these limits vary approximately $10 \text{ GeV}/c^2$ if \tilde{t}_1 and/or sleptons are light.

III. SEARCH FOR DIRAC MONOPOLES

One of the open questions of particle physics is the existence of Dirac monopoles [13,14], hypothetical carriers of the magnetic charge proposed by P.M. Dirac to symmetrize Maxwell equations and explain the quantization of electric charge. If such magnetic monopoles exist, then the elementary magnetic and electric charges (g and e) must be quantized according to the following formula:

$$g = \frac{2\pi n}{e}, \quad n = \pm 1, \pm 2, \dots, \quad (1)$$

where n is an unknown integer.

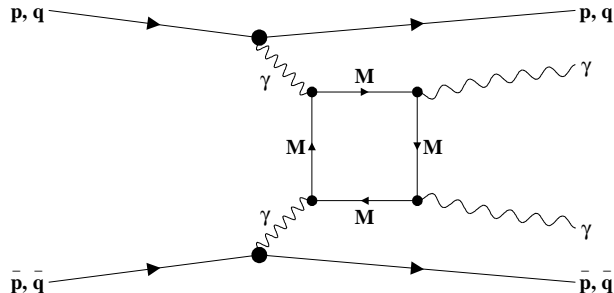


FIG. 4. Feynman diagram for $\gamma\gamma$ production via a virtual monopole loop.

Dirac monopoles are expected to couple to photons with a coupling constant $\alpha_g = g^2/4\pi \approx 34 n^2$ which is at least three orders of magnitude larger than the corresponding photon coupling to the electric charge ($\alpha_e = e^2/4\pi \approx 1/137$). Therefore such monopoles could give rise to photon-photon rescattering via the box diagram shown in Fig. 4 [15,16]. The contribution of this diagram for pointlike monopoles to diphoton production at hadron colliders was recently calculated [17] and shown to be significant even for monopole masses comparable to the collider beam energy.

Since the virtuality (Q^2) of most incoming photons in the process of Fig. 4 is small [18], the interacting partons scatter at very small angles and therefore escape the detector through the beam pipe. Thus, a signature for monopoles at hadron colliders is the production of a pair of isolated photons with high transverse energies. This process gives a unique opportunity to find evidence for Dirac monopoles or to set limits on the monopole mass. Previous monopole searches can be found in Ref. [19,20].

Despite numerous studies, QED with pointlike monopoles is still not a complete theory. For example, it is not clear whether such a theory can be constructed to be renormalizable to all orders [16]. Also, arguments exist (see, e.g. [21]) that Dirac monopoles must occupy a spatial volume of radius $R \sim \mathcal{O}(g^2/M)$, where M is the monopole mass, to accommodate the self energy implied by the large coupling. In such a theory, it is possible that hard interactions of a monopole with photons would be weakened substantially by the effects of a monopole form factor.

The data used in this analysis represent an integrated luminosity of $69.5 \pm 3.7 \text{ pb}^{-1}$ using a trigger which required the presence of an electromagnetic object with transverse energy E_T above 40 GeV. This trigger did not require the presence of an inelastic collision, and therefore can be used to select low Q^2 events typical of the process in Fig. 4.

The following offline selection criteria are: (i) at least two photons with $E_T > 40 \text{ GeV}$ and pseudorapidity $|\eta^\gamma| < 1.1$; (ii) missing transverse energy in the event $\cancel{E}_T < 25 \text{ GeV}$; and (iii) no jets with $E_T^j > 15 \text{ GeV}$ and $|\eta^j| < 2.5$. The jet veto requirement is used to select the low Q^2 process in Fig. 4. The trigger is $> 98\%$ efficient for this off-line selection.

Photons are selected from the identified EM clusters by requiring no tracks pointing toward the cluster from any of the event vertices. The overall efficiency for photon identification is $(73.0 \pm 1.2)\%$ per photon. The total efficiency for diphoton is $(52.8 \pm 1.4)\%$. This includes the efficiency of the \cancel{E}_T veto $(99.0 \pm 0.5)\%$ as well as the identification efficiency for a pair of photons. The above selection criteria define our base sample which contains 90 candidate events.

The main backgrounds to photon scattering through a monopole loop are due to: (i) diagrams similar to Fig. 4 with other particles in the loop; (ii) QCD production of dijets (jj) and direct photons ($j\gamma$) (with jets misidentified as photons due to fragmentation into a leading π^0 or η decaying into a pair of spatially close photons, reconstructed as one EM cluster), or direct diphotons ($\gamma\gamma$); and (iii) Drell-Yan dielectron production with electrons misidentified as photons due to tracking inefficiency.

Background (i) is dominated by a virtual W -loop and has been shown to be negligible [22]. The other two background contributions are estimated from the data. The QCD background is determined using the $j\gamma$ event sample collected with a single photon trigger, with the jet passing the same fiducial and kinematic cuts as the photon. By applying a jet-faking probability, we find the QCD background to be 25 ± 8 events. Direct photon and diphoton backgrounds are also included in this estimate.

The Drell-Yan background is calculated from a sample of dielectron events passing the same fiducial and kinematic cuts as the signal sample. Multijet contamination of this sample is negligible. The probability for a dielectron pair to be misidentified as a diphoton pair is found to be $(11 \pm 1)\%$ by comparing the number of events in the Z peak in the ee and $\gamma\gamma$ samples passing loose kinematic cuts. The Drell-Yan background in the base sample is 63 ± 7 events. The overall background in the base sample is 88 ± 11 (syst) events, in good agreement with the 90 observed candidates.

To optimize the sensitivity of this search to the monopole loop contribution we apply a cut on the scalar sum of the transverse energies of all the photons in the event: $S_T \equiv \sum_i E_T^{\gamma_i}$. We vary the S_T cut threshold (S_T^{\min}) in 10 GeV steps to achieve an expected background of 0.4 events. Such an optimization is based on the fact that for this expected background one has a 67% probability of observing no candidate events in the data in the absence of a

signal. In such a case [20], the limits on the signal do not depend on the exact background value or its uncertainties. The agreement between the observed number of events and the predicted background as a function of S_T^{\min} is illustrated in Fig. 5. The $S_T^{\min} = 250$ GeV cut corresponds to a background of 0.41 ± 0.11 events. We set an upper limit for the production cross section of two or more photons with $\sum E_T^\gamma > 250$ GeV and $|\eta^\gamma| < 1.1$:

$$\sigma(p\bar{p} \rightarrow \geq 2\gamma) |_{S_T > 250 \text{ GeV}, |\eta^\gamma| < 1.1} < 83 \text{ fb} \quad (2)$$

at the 95% C.L.

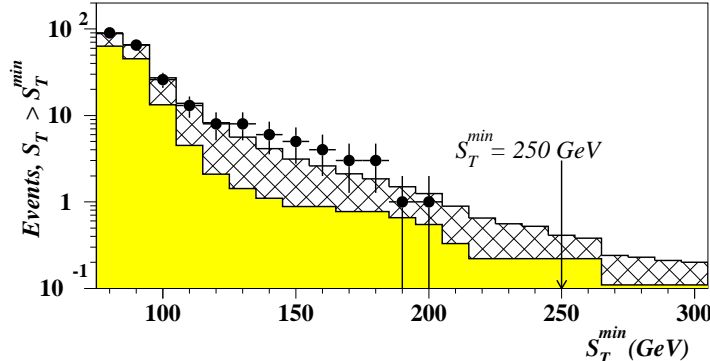


FIG. 5. Data and expected background as a function of S_T^{\min} cut. Points are data, the upper hatched region corresponds to the QCD background, and the lower shaded region shows the Drell-Yan background. The $\approx 15\%$ systematic error on the background is not shown.

Since the data are consistent with the background hypothesis, we can set limits on the production of pointlike Dirac monopoles. We calculate the acceptance for the monopole signal using a fast MC program that generates diphoton events from a monopole loop according to the calculated differential cross section $d^3\sigma/dE_T^\gamma d\eta^{\gamma 1} d\eta^{\gamma 2}$ [17] with a subsequent parametric simulation of the DØ detector. The overall acceptance for the monopole signal is found to be $(51 \pm 1)\%$. The acceptance does not depend on the monopole mass for masses above the typical photon energy (~ 300 GeV) [18].

The total cross section for heavy monopole production at the Tevatron is given by [17]:

$$\sigma(p\bar{p} \rightarrow \gamma\gamma + X) = 57 P \left(\frac{n}{M \text{ [TeV]}} \right)^8 \text{ fb}, \quad (3)$$

where P is a spin dependent factor [22,23]: $P = 0.085, 1.39$, and 159 for monopole spin of $0, 1/2$, and 1 , respectively. The estimated error on this cross section due to choice of p.d.f. and to higher order QED effects is 30% [18]. Additional uncertainties are associated with the $\gamma\gamma \rightarrow \gamma\gamma$ subprocess in Fig. 4 and with unitarity considerations. The coupling constant α_g is replaced with an effective coupling [17] obtained by multiplying α_g by a factor $(E^\gamma/M)^2$, where E^γ is the photon energy, typically 300 GeV at the Tevatron. Both unitarity and perturbation theory assumptions are satisfied when this factor is $\ll 1$ [15,17].

Comparing the lower bound of the theoretical cross section corrected for acceptance with the cross section limit set by this measurement, we obtain the following lower limits on the

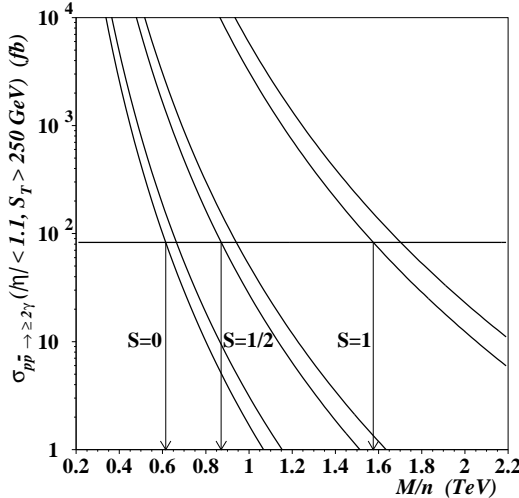


FIG. 6. The curved bands show the low and upper bounds on theoretical cross sections [17] for monopole spin, $S = 0, 1/2$, and 1 . The horizontal line shows the 95% C.L. experimental upper limit on the cross section. The arrows indicate the lower 95% C.L. limits on the monopole mass at each spin value.

pointlike Dirac monopole mass (see Fig. 6):

$$M/n > \begin{cases} 610 \text{ GeV for } S = 0 \\ 870 \text{ GeV for } S = 1/2 \\ 1580 \text{ GeV for } S = 1 \end{cases} .$$

We note that the effective coupling exceeds 1 and unitarity is violated close to the experimental bound. For values $E^\gamma/M > 1$, the cross section will grow more slowly, approaching the usual $1/M^2$ behavior of a QED process [18] which satisfies unitarity. Also, for lower monopole masses the effective parameter of the perturbation theory used in the calculations [17] becomes too large, and therefore one would expect a non-negligible contribution of the higher order diagrams with four, six, etc. photons in the final state. The latter effect is, however, largely compensated by our analysis cut on the sum of the photon transverse energies; if part of the signal cross section is due to the higher order diagrams, the above limits are unaffected.

IV. SUMMARY

In summary, we have performed searches for supersymmetry by searching for $\gamma\gamma E_T$ and $\gamma E_T + \geq 2$ jets events and for heavy pointlike Dirac monopoles by searching for pairs of photons with high transverse energies. Our data agree with the expected background production. Within the framework of the MSSM with the choices of the parameter values consistent with $\text{Br}(\tilde{\chi}_2^0 \rightarrow \gamma\tilde{\chi}_1^0) = 100\%$ and $m_{\tilde{\chi}_2^0} - m_{\tilde{\chi}_1^0} > 20 \text{ GeV}/c^2$, we obtain a 95% C.L. lower mass limit of $311 \text{ GeV}/c^2$ for equal mass squarks and gluinos. Using theoretical calculations [17] we set 95% C.L. lower limits on the Dirac monopole mass for minimum magnetic charge ($n = 1$) in the range 610 to 1580 GeV, depending on the monopole spin.

[1] DØ Collaboration, S. Abachi *et al.*, Nucl. Instrum. Methods A **338**, 185 (1994).

[2] For a review, see for example: H.E. Haber and G. Kane, Phys. Rept. **117**, 75 (1985).

[3] S. Dimopoulos, S. Thomas, and J.D. Wells, Phys. Rev. D **54**, 3283 (1996); S. Dimopoulos *et al.*, Phys. Rev. Lett. **76**, 3494 (1996); K.S. Babu, C. Kolda, and F. Wilczek, Phys. Rev. Lett. **77**, 3070 (1996); J.L. Lopez, D.V. Nanopoulos, and A. Zichichi, Phys. Rev. Lett. **77**, 5168 (1996); S. Ambrosanio *et al.*, Phys. Rev. D **54**, 5395 (1996); H. Baer *et al.*, Phys. Rev. D **55**, 4463 (1997); J. Ellis, J.L. Lopez, and D.V. Nanopoulos, Phys. Lett. B **394**, 354 (1997).

[4] S. Ambrosanio *et al.*, Phys. Rev. Lett. **76**, 3498 (1996) and Phys. Rev. D **55**, 1372 (1997).

[5] CDF Collaboration, F. Abe *et al.*, [hep-ex/9801019](#), submitted to Phys. Rev. Lett.

[6] S. Ambrosanio and B. Mele, Phys. Rev. D **55**, 1399 (1997), Erratum-ibid. D **56**, 3157 (1997).

[7] DØ Collaboration, B. Abbott *et al.*, Phys. Rev. Lett. **80**, 442 (1998).

[8] F.E. Paige and S.D. Protopopescu, BNL report No. BNL38034 (1986) (unpublished).

[9] DØ Collaboration, S. Abachi *et al.*, Phys. Rev. Lett. **78**, 2070 (1997).

[10] H.U. Bengtsson and T. Sjöstrand, Comp. Phys. Comm. **46**, 43 (1987); T. Sjöstrand, Comp. Phys. Comm. **82**, 74 (1994); S. Mrenna, Comp. Phys. Comm. **101**, 232 (1997).

[11] H. L. Lai *et al.*, Phys. Rev. D **51**, 4763 (1995).

[12] DØ Collaboration, S. Abachi *et al.*, Phys. Rev. Lett. **76**, 2222 (1996); A. Kounine, “*Higgs and Supersymmetry Searches at LEP*”, see this proceeding.

[13] P.A.M. Dirac, Proc. R. Soc. London, Ser. A **133**, 60 (1931).

[14] J. Schwinger, Phys. Rev. **151**, 1055 (1966).

[15] I.F. Ginzburg, S.L. Panfil, Sov. J. Nucl. Phys. **36**, 850 (1982).

[16] A. De Rújula, Nucl. Phys. **B435**, 257 (1995).

[17] I.F. Ginzburg and A. Schiller, [hep-ph/9802310](#), To appear in Phys. Rev. D.

[18] I.F. Ginzburg, private communication.

[19] L3 Collaboration, M. Acciarri *et al.*, Phys. Lett. B **345**, 609 (1995).

[20] PDG Review of Particle Physics, Phys. Rev. D **54**, 166, 685-687 (1996).

[21] A.S. Goldhaber, in Proceedings of the CRM–FIELDS–CAP Workshop “Solitons” at Queen’s University, Kingston, Ontario, July 1997 (Springer, New York 1998).

[22] G. Jikia and A. Tkabladze, Phys. Lett. B **323**, 453 (1994).

[23] W. Heisenberg and H. Euler, Z. Phys. **38**, 714 (1936); V. Constantini, B. De Tollis, and G. Pistoni, Nuovo Cim. **2A**, 733 (1971); M. Baillagreton, G. Belanger, and F. Boudjema, Phys. Rev. D **51**, 4712 (1995); M. Baillagreton, F. Boudjema, E. Chopin, and V. Lafage, Z. Phys. C **67**, 431 (1996).